High Resolution Compton Scattering in Fermi Surface Studies: Application to FeAl

C. Blaas and J. Redinger
Institut für Technische Elektrochemie, Technische Universität Wien, Getreidemarkt 9/158, A-1060 Wien, Austria

S. Manninen, V. Honkimäki, and K. Hämäläinen
Department of Physics, University of Helsinki, P.O. Box 9, FIN-00014 Finland

P. Suortti
European Synchrotron Radiation Facility, B.P. 220, F-38043 Grenoble, France
(Received 31 March 1995)

We present a novel theoretical approach to identify Fermi surface contributions in high resolution Compton scattering data. For FeAl Compton profiles we show that the Fermi-surface-related features (occupation of states) can be separated from those originating from the spatial extent of the wave functions. The first high resolution Compton scattering experiment done at the European Synchrotron Radiation Facility confirms these findings. This technique opens up new possibilities especially in Fermiology studies of high temperature superconductors.

PACS numbers: 71.25.Pi, 41.60.Ap, 78.70.Ck

Compton scattering studies provide a rather direct access to both spatial extent and occupation (Fermi surface) of the electronic ground-state wave functions in terms of the electron momentum density (EMD). Within the impulse approximation [1,2] the Compton profile (CP) is the projection of the EMD onto the scattering vector. The Compton line shape is very sensitive to the behavior of the valence electrons and provides a basis to test not only the band-theory wave functions, but also the underlying one-electron approximations [3,4]. Clearly, one would prefer to compare experiment and theory on the basis of the EMD itself, as the projection seen in the experimentally accessible CP's allows one only to identify structures in the EMD averaged over the planes perpendicular to the scattering vector. Therefore, if reconstruction techniques for the EMD are not applicable, it is of prime importance to use an approach which is capable of extracting the relevant Fermi-surface-related aspects from Compton data alone. In this Letter we apply such an approach to FeAl and demonstrate that the different Fermi surface cross sections involved in the projection of the EMD are responsible for prominent structures in directional CP's and their differences.

The EMD is a single-centered function and shows the point-group symmetry of the underlying space group. In metals the Fermi surface plays a crucial role, i.e., only those parts of momentum space are occupied which lie inside the Fermi volumes repeated at each reciprocal lattice point. Hence the EMD will show discontinuities at the positions of the Fermi surface. Whether or not such a Fermi break can be observed in the EMD at a particular momentum value depends on the observability rules as discussed by Harthoorn and Mijnarends for the symmorphic cubic groups [5]. The location of these Fermi breaks provides information on the topology of the Fermi surface, the size of the discontinuity allows discussion of correlation effects (renormalization of the Landau quasiparticle), while information concerning the wave functions may be obtained from the overall shape of the EMD.

Compared with alternative methods for Fermi surface studies, such as angular correlation of positron annihilation or de Haas–van Alphen techniques, Compton scattering offers several advantages. The results are not sensitive to the sample purity or to lattice defects, and low temperature measurements are not required. The limiting factor so far has been the resolution, but modern crystal spectrometers at the third generation synchrotron sources have overcome this problem.

The first period transition metals form interesting alloys with aluminum covering the entire concentration range. The ordered equiatomic alloy FeAl crystallizes in the simple CsCl-type crystal structure. Great efforts have been made to study the character of bonding and the charge transfer in this alloy. Earlier Compton scattering studies were made with low resolution by Chaddah and Sahni [6] and Manninen *et al.* [7] using polycrystalline samples, hence making the analysis of the anisotropies impossible. Podloucky and Neckel [8] used a quasi-self-consistent augmented plane-wave method and found a remarkable anisotropy, which should easily be seen even in low resolution experiments.

The FeAl single crystals used in the experiment were grown by the Bridgman method. Slices of equal thickness were cut along the (100) and (111) planes by electroerosion. A Laue photograph was then used to check the orientation. Preliminary experiments were first made by using a conventional spectrometer based on monochromatic W $K\alpha_1$ radiation (59.3 keV) and a solid state detector. Since the resolution of this experiment (0.55 a.u.) was not good

 0031-9007/95/75(10)/1984(4)$06.00

enough to see details in the momentum anisotropy, these measurements served to check the performance of the high resolution spectrometer as far as the gross features are concerned.

The high resolution spectrometer at the European Synchroton Radiation Facility (ESRF) beamline BL25 (ID15) was used in the actual experiment [9]. Radiation from the multipole wiggler (critical energy 43 keV) was monochromatized using a horizontally focusing Bragg-type bent Si(220) crystal. A photon energy of 49.6 keV was used in the experiment. The scattered energy spectrum was analyzed using a bent focusing Ge(440) crystal followed by a NaI(Tl) scintillation counter both moving simultaneously on the focusing circle. The resolution function of the spectrometer was both calculated as a function of the energy and measured using a Gd sample, which has a K fluorescence line (43 keV) close to the Compton peak center. Both methods gave roughly the same result, about 95 eV, at the Compton peak. In terms of the momentum resolution this corresponds to 0.15 a.u., which is good enough to see the details predicted by theory. In this type of spectrometer the resolution is limited by the irradiated sample volume seen by the detector (optical source size). The absorption in FeAl is slightly smaller than in the Gd sample. This difference is taken into account when the experimental results are compared with the theory.

One hour scans repeated during two full shifts of 8 h were used for both crystal directions. Altogether about 1.5×10^7 counts were collected for both samples. A monitor counter (Ge solid state detector) measuring the Compton scattering from the sample was used to correct the fluctuations in the primary beam intensity. The measured spectra were corrected for the background and the effects depending on the energy and the geometry, converted to the momentum scale, and finally normalized to the theoretical values within the momentum range of ± 6 a.u. No correction was made for multiple scattering effects. Based on a Monte Carlo calculation the multiple scattering contribution was about 10% in the case of the conventional spectrometer results. Because of the linear polarization of the synchrotron radiation, the amount of multiple scattering decreases [10] and the major part of this smooth and in the first approximation isotropic contribution is already subtracted with the background contribution, which affects the normalization of the profiles (multiple scattering is included in the normalization). The remaining effect is within the statistical error bars.

The comparison between experiment and theory is more reliable in terms of differences between directional Compton profiles (DCP's). Providing that the sample thicknesses and the measuring geometries are identical, most of the remaining systematic errors cancel out when the difference is taken. In particular, the core electron contribution, which is large in the case of high Z materials, cancels out as well.

The calculations were performed at the experimental lattice constant $a = 5.496\,19$ a.u. for FeAl using the all-electron full potential linearized augmented plane wave (FLAPW) method [11]. Exchange and correlation effects were treated strictly within the local density approximation (LDA). A practical method for calculating CP's for cubic systems has been described by Blaas *et al.* [12]. In this scheme, both EMD and CP's are represented in terms of multipole expansions. The EMD coefficients are obtained by a Gaussian projection from a set of special directions, and the corresponding CP coefficients are computed by a one-dimensional integration involving the EMD coefficients. The valence EMD was obtained by a quasianalytical Fourier inversion of the FLAPW wave functions and subsequent squaring for a momentum interval of $0.01(\frac{2\pi}{a})$ with a maximum value of $6.5(\frac{2\pi}{a})$ along each of the 45 special directions [13,14] determining the expansion coefficients up to $l = 48$. Beyond $6.5(\frac{2\pi}{a})$ only the isotropic part was considered, which is enough to ensure the correct norm of the valence EMD (CP's). The total CP's were determined by adding an atomiclike core contribution and a Lam-Platzman term [15] (isotropic in the LDA), which corrects for residual electron correlation effects missing in the EMD calculated from one-electron Kohn-Sham orbitals.

In Fig. 1 the DCP [100]-[111] for FeAl resulting from the experiment using a conventional W $K\alpha_1$ x-ray spectrometer (a) and from the first high resolution Compton scattering experiment at the ESRF (b) are shown. This figure demonstrates impressively the potential of high resolution Compton scattering experiments. The low resolution x-ray data yield only broad features in fair agreement with theory, while in the high resolution data important new structures show up. Theory and ESRF experiments already come very close. There are no finer structures hidden in the unconvoluted theory as can be seen by comparing Figs. 1(b) and 1(c). It is only the magnitude of the minima and maxima which is affected by the experimental resolution. It is worthwhile to note that the distance between the maxima (minima) as seen in the low resolution x-ray experiment is about the size of one Brillouin zone. The additional structures as seen by the high resolution Compton scattering experiment have a much smaller pitch, indicating regular changes in the EMD happening on a scale that is smaller than one Brillouin zone. In the following discussion it will be shown for the first time that these new features are heavily influenced by the shape of the particular Fermi surface.

The 11 valence electrons of FeAl require six bands. The three lowest bands (one Al s-like and two Fe d-like) are always filled completely. The fourth, fifth, and sixth bands (all Fe d-like) are filled partially with 1.95, 1.80, and 1.25 electrons, respectively. These bands span the three sheets of the Fermi surface. Roughly speaking, the almost filled fourth and fifth bands have unoccupied

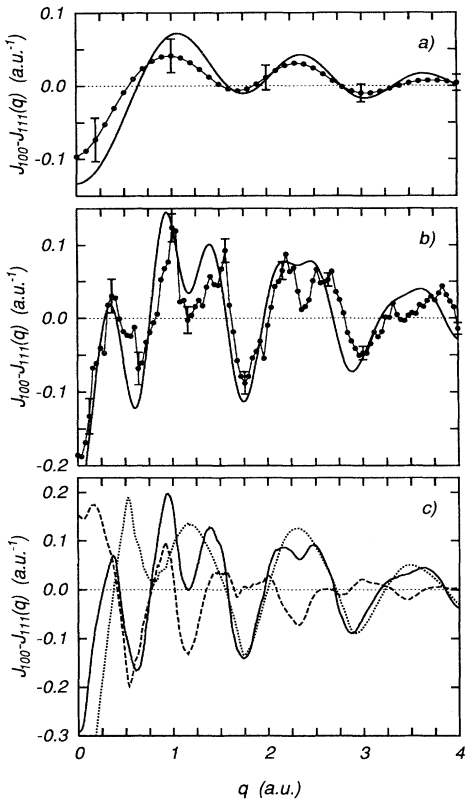

FIG. 1. Experimental and theoretical difference Compton profile [100]-[111] for FeAl: (a) low resolution x-ray (W $K\alpha_1$) experiment (bullets), theory convoluted with appropriate W $K\alpha_1$ resolution function (solid). (b) Present high resolution ESRF experiment (bullets), theory convoluted with the ESRF resolution function (solid). For both experimental data sets the estimated error bars are drawn. (c) Fermi-surface-induced variations (unconvoluted theory): difference Compton profile (solid), difference Compton profile with six bands assumed to be filled completely, i.e., the Fermi surface is removed (dotted), and influence of the sixth band Fermi surface, i.e., the difference between a partially filled and a completely filled sixth band (dashed).

holes around Γ and R points of the simple-cubic Brillouin zone. The sixth band sheet shows the most pronounced topology adding electrons in regions around M points and thereby forming a multiply connected monster (cross sections through the Fermi surface of this band can be seen in Fig. 3).

In theory it is possible to remove all Fermi surface topology related features by completing the partially filled bands. Additionally, it is possible to analyze the CP's in terms of the contributions from the individual bands. Figure 1(c) stresses those features in the DCP [100]-[111], which depend on the Fermi surface topology, by comparing the DCP of FeAl with a synthetic DCP resulting if all six bands are assumed to be filled completely, i.e., the regions of momentum space outside the Fermi volumes have been refilled. A significant effect is seen for momentum values $q < 0.75$ a.u., leading to a pronounced minimum around $q = 0.6$ a.u. This minimum has to be attributed to all three sheets of the Fermi surface with the largest contribution due to the sixth band. The Fermi surface of the sixth band [its influence is shown as a dashed line in Fig. 1(c)] is also responsible for the double peak structures around $q = 1.2$, 2.3, and 3.4 a.u., while the fourth and fifth bands give only very small contributions. These structures are only revealed by the high resolution ESRF experiment.

Two reasons for the occurrence of minima and maxima in DCP's are possible. The directional anisotropy caused by the spatial extent of the wave functions will always show up and generate broad features; i.e., the overall shape of the DCP in Fig. 1 for $q > 0.75$ a.u. is attributed to the e_g/t_{2g}-like anisotropy of the FeAl d-like wave functions. But structures originating from the directional dependence of the Fermi surface may be seen as well. Hence it is important to find out how the Fermi surface influences the individual directional CP's. For FeAl we expect the strongest effects for [100], because for a simple-cubic lattice cross sections with the plane of integration perpendicular to [100] at a given q are the same for all Fermi volumes cut through by this plane. For other directions the plane of integration at a given q cuts through several different portions of the Fermi volumes. Hence, the modulation along q when the cross sections are summed over the integration planes is less pronounced than for [100], for which only identical areas are summed up.

In Fig. 2 we show the valence CP [100] and the synthetic CP, which results from assuming six completely filled bands. Additionally, the difference between these two CP's indicating the presence of the Fermi surface is shown for each of the three sheets of the Fermi surface. Obviously, the Fermi-surface-induced modifications are of the same order of magnitude as amplitudes in DCP's. Again, the changes due to the sixth band dominate and form a periodic pattern. The changes originating from the fourth and fifth bands follow that pattern. The line shape of the CP [100] can be understood in terms of the passage of the plane of integration through the Fermi volumes centered at reciprocal lattice points. The extremal cross sections through the Fermi surface of the sixth band are shown in Fig. 3. The CP [100] has bumps at q values labeled (b) corresponding to the largest occupied Fermi surface cross section located about half way between the Brillouin zone center at Γ and the Brillouin zone boundary at X. The dents in the CP [100] seen at q values labeled (a) and (c) are caused by their corresponding Fermi surface cross sections shown in Fig. 3. Although cross sections (a) and (c) are of similar size, those at (a) reflect cuts through the zone centers, whereas those at (c) cuts through zone boundaries. It is precisely this periodically repeated (b)(a)(b) structure

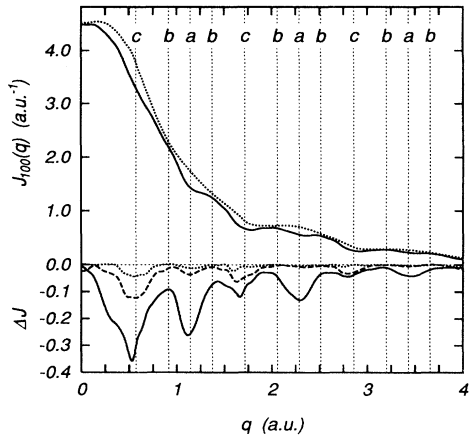

FIG. 2. Upper panel: theoretical valence Compton profile [100] for FeAl (solid), synthetic valence Compton profile [100] with six bands assumed to be filled completely, i.e., full d bands and no Fermi surface (dotted). Lower panel: Fermi-surface-induced effects for individual bands, i.e., differences between partially filled and assumed completely filled bands: fourth band (dotted), fifth band (dashed), sixth band (solid). The q values for which the Fermi-surface-induced variations show extremal behavior are indicated by vertical lines labeled a, b, and c (see Fig. 3).

which produces the dips seen in the DCP [100]-[111] in Fig. 1 at $q = 1.2$, 2.3, and 3.4 a.u., as the CP [111] is indeed less affected by the Fermi surface. For momentum values $q < 0.6$ a.u. the regular pattern of the Fermi surface induced changes in Fig. 2 is disrupted, which is a consequence of the EMD observability rules [5] imposing their strongest restrictions throughout planes close to the origin overriding the Fermi-surface-induced effects.

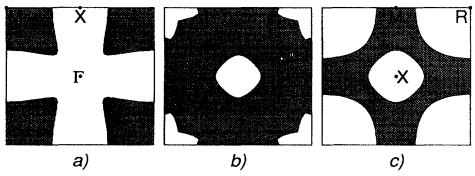

FIG. 3. Intersections of the Fermi surface of the sixth band in FeAl with planes perpendicular to [100] at various distances q from the origin (occupied areas are shaded): (a) $q = 0$, 1, 2, $3\,(\frac{2\pi}{a}), \ldots$, (b) $q = 0.2$, 0.8, 1.2, 1.8, 2.2, 2.8, $3.2\,(\frac{2\pi}{a}), \ldots$, (c) $q = 0.5$, 1.5, $2.5\,(\frac{2\pi}{a}), \ldots$. The labels Γ, R, M, X indicate the high-symmetry points of the simple-cubic Brillouin zone. The calculation of the Compton profile [100] at a given q involves an integration over the occupied (shaded) areas periodically repeated in the plane.

Summarizing, we have observed that the shape of the Fermi surface represented by its different cross sections leaves a clear mark on directional CP's and on the differences between them. High resolution Compton scattering as done at the ESRF is able to reveal these marks experimentally. One may say that it has established itself to be a powerful tool in Fermiology studies without the necessity of high quality single crystals or very low temperatures. The techniques discussed in this Letter will be applicable for a large variety of systems with complex Fermi surfaces such as high temperature superconductor materials.

We wish to thank Professor S. G. Steinemann, University Lausanne/Switzerland, for providing the samples and Dr. P. Marksteiner, University Vienna Computing Center, for his kind help in determining the Gaussian directions. We would also like to thank R. Karhumaa, J. Laukkanen, and J. E. McCarthy for assistance during the experiments. The present work was supported by the Academy of Finland (Contract No. 8582). One of the authors (C. B.) would like to acknowledge financial support from the International Center for Computational Materials Science in Vienna.

[1] P. M. Platzman and N. Tzoar, Phys. Rev. **139**, 410 (1965).
[2] P. Eisenberger and P. M. Platzman, Phys. Rev. A **2**, 415 (1970).
[3] G. E. W. Bauer and J. R. Schneider, Phys. Rev. Lett. **52**, 2061 (1984).
[4] G. E. W. Bauer and J. R. Schneider, Phys. Rev. B **31**, 681 (1985).
[5] R. Harthoorn and P. M. Mijnarends, J. Phys. F **8**, 1147 (1978).
[6] P. Chaddah and V. C. Sahni, Philos. Mag. B **37**, 305 (1978).
[7] S. Manninen, B. K. Sharma, T. Paakkari, S. Rundqvist, and M. W. Richardsson, Phys. Status Solidi B **107**, 749 (1981).
[8] R. Podloucky and A. Neckel, Phys. Status Solidi B **95**, 541 (1979).
[9] S. Manninen *et al.* (to be published).
[10] F. Bell and J. Felsteiner (to be published).
[11] H. J. F. Jansen and A. J. Freeman, Phys. Rev. B **30**, 561 (1984).
[12] C. Blaas, J. Redinger, R. Podloucky, P. Jonas, and P. Schattschneider, Z. Naturforsch. A **48**, 198 (1993).
[13] W. R. Fehlner and S. H. Vosko, Can. J. Phys. **54**, 2159 (1976).
[14] P. Marksteiner (private communication).
[15] L. Lam and P. M. Platzman, Phys. Rev. B **9**, 5122 (1974).